arXiv:2305.15241v1 [cs.CV] 24 May 2023

Robust Classification via a Single Diffusion Model

Huanran Chen[1,2], **Yinpeng Dong**[1], **Zhengyi Wang**[1], **Xiao Yang**[1], **Chengqi Duan**[1], **Hang Su**[1], **Jun Zhu**[1]
[1]Dept. of Comp. Sci. and Tech., Institute for AI, Tsinghua-Bosch Joint ML Center, THBI Lab, BNRist Center, Tsinghua University, Beijing, 100084, China
[2]School of Computer Science, Beijing Institute of Technology
huanranchen@bit.edu.cn,
{dongyinpeng, wang-zy21, yangxiao19, duancq20, suhangss, dcszj}@mail.tsinghua.edu.cn

Abstract

Recently, diffusion models have been successfully applied to improving adversarial robustness of image classifiers by purifying the adversarial noises or generating realistic data for adversarial training. However, the diffusion-based purification can be evaded by stronger adaptive attacks while adversarial training does not perform well under unseen threats, exhibiting inevitable limitations of these methods. To better harness the expressive power of diffusion models, in this paper we propose Robust Diffusion Classifier (RDC), a generative classifier that is constructed from a pre-trained diffusion model to be adversarially robust. Our method first maximizes the data likelihood of a given input and then predicts the class probabilities of the optimized input using the conditional likelihood of the diffusion model through Bayes' theorem. Since our method does not require training on particular adversarial attacks, we demonstrate that it is more generalizable to defend against multiple unseen threats. In particular, RDC achieves 73.24% robust accuracy against ℓ_∞ norm-bounded perturbations with $\epsilon_\infty = 8/255$ on CIFAR-10, surpassing the previous state-of-the-art adversarial training models by $+2.34\%$. The findings highlight the potential of generative classifiers by employing diffusion models for adversarial robustness compared with the commonly studied discriminative classifiers.

1 Introduction

A longstanding problem of deep learning is the vulnerability to adversarial examples [18, 51], which are maliciously generated by adding human-imperceptible perturbations to natural examples, but can cause deep learning models to make erroneous predictions. Since the adversarial robustness problem leads to security threats in real-world applications (e.g., face recognition [14, 44], autonomous driving [4, 24], healthcare [16]), there has been a lot of work on defending against adversarial examples, such as adversarial training [18, 34, 61], image denoising [32, 42, 48], certified defenses [8, 38, 56].

Recently, diffusion models have emerged as a powerful family of generative models, consisting of a forward diffusion process that gradually perturbs data with Gaussian noises and a reverse generative process that learns to remove noise from the perturbed data [23, 36, 45, 49]. Some researchers have tried to apply diffusion models to improving adversarial robustness in different ways. For example, the adversarial images can be purified through the forward and reverse processes of diffusion models before feeding into the classifier [3, 37, 54]. Besides, the generated data from diffusion models can significantly improve adversarial training [40, 55], achieving the state-of-the-art results on robustness benchmarks [10]. These works show promise of diffusion models in the field of adversarial robustness.

However, there are still some limitations of the existing methods. On one hand, the diffusion-based purification approach is a kind of gradient obfuscation [1, 17], and can be effectively attacked by using

Preprint. Under review.

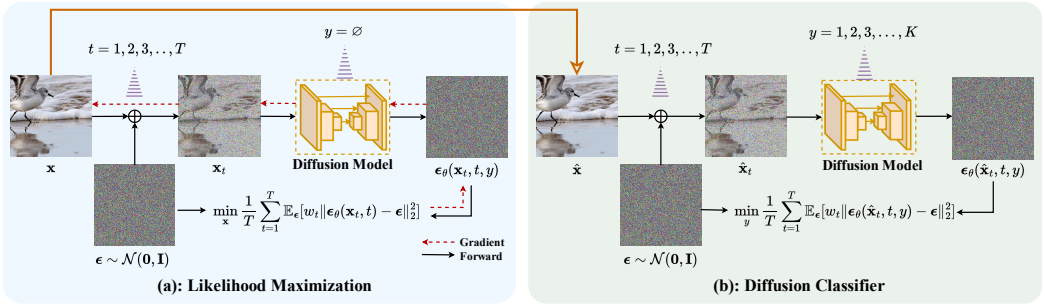

Figure 1: Illustration of our proposed Robust Diffusion Classifier (RDC). Given an input image $\mathbf{x}$, our approach first maximizes the data likelihood (Left) and then classifies the optimized image $\hat{\mathbf{x}}$ with a diffusion model (Right). The class probability $p(y|\hat{\mathbf{x}})$ is given by the conditional log-likelihood $\log p_\theta(\hat{\mathbf{x}}|y)$, which is approximated by the variational lower bound involving calculating the noise prediction error (i.e., diffusion loss) averaged over different timesteps for every class.

the exact gradient and a proper step size[1]. We observe that the adversarial example cannot make the diffusion model output an image of a different class, but the perturbation is not completely removed. Therefore, the poor robustness of diffusion-based purification is largely due to the vulnerability of downstream classifiers. On the other hand, although adversarial training methods using data generated by diffusion models achieve excellent performance, they are usually not generalizable across different threat models [28, 52]. In summary, these methods leverage diffusion models to improve adversarial robustness of discriminative classifiers, but discriminative learning cannot capture the underlying structure of data distribution, making it hard to control the predictions of inputs outside the training distribution [43]. As a generative approach, diffusion models have more accurate score estimation (i.e., gradient of log-density at the data point) in the whole data space [23, 47, 49], which also have the potential to provide accurate class probabilities. Therefore, we try to explore *how to convert a diffusion model into a generative classifier for improved adversarial robustness?*

In this paper, we propose **Robust Diffusion Classifier (RDC)**, a generative classifier obtained from a single off-the-shelf diffusion model to achieve adversarial robustness, as shown in Fig. 1. Our method estimates the class probability $p(y|\mathbf{x})$ by using the conditional likelihood $p_\theta(\mathbf{x}|y)$ of a diffusion model with a prior distribution $p(y)$ through Bayes' theorem. The conditional likelihood is approximated by the variational lower bound, which involves calculating the noise prediction loss for every class under different noise levels. Theoretically, we validate that the optimal diffusion model can achieve absolute robustness under common threat models. However, the practical diffusion model may have an inaccurate density estimation $p_\theta(\mathbf{x}|y)$ or a large gap between the likelihood and its lower bound, leading to inferior performance. To address this issue, we further propose a likelihood maximization method as a pre-optimization step to move the input data to regions of high likelihoods before feeding into the diffusion classifier. Therefore, our proposed RDC, directly constructed from a pre-trained diffusion model without training on specific adversarial attacks, can perform robust classification under various threat models.

We empirically compare our proposed method with various state-of-the-art methods against strong adaptive attacks on CIFAR-10 [26]. In particular, RDC achieves 73.24% robust accuracy under the ℓ_∞ norm threat model with $\epsilon_\infty = 8/255$, exhibiting a $+2.34\%$ improvement over the state-of-the-art adversarial training method [55]. Under unseen threats, RDC leads to a more significant improvement ($> 30\%$) over adversarial training models and DiffPure [37]. We further conduct thorough analysis of more carefully-designed adaptive attacks and various ablation studies to verify that the achieved robustness is not caused by gradient obfuscation [1]. Our findings disclose the potential of generative models for solving the adversarial robustness problem.

[1]We lower the robust accuracy of DiffPure [37] from 71.29% to 53.52% under the ℓ_∞ norm with $\epsilon_\infty = 8/255$, and from 80.60% to 75.98% under the ℓ_2 norm with $\epsilon_2 = 0.5$, as shown in Table 1.

2 Related work

Adversarial robustness. Adversarial examples [18, 51] are widely studied in the literature, which are generated by adding imperceptible perturbations to natural examples, but can mislead deep learning models. Many adversarial attack methods [1, 5, 9, 12, 13, 34] have been proposed to improve the attack success rate under the white-box or black-box settings, which can be used to evaluate model robustness. To defend against adversarial attacks, adversarial training [34, 40, 61] stands out as the most effective method, which trains neural networks using adversarially augmented data. However, these models tend to exhibit robustness only to a specific attack they are trained with, and have poor generalization ability to unseen threats [28, 52]. Another popular approach is adversarial purification [32, 37, 42, 48], which denoises the input images for classification. Most of these defenses cause obfuscated gradients [1] and can be evaded by adaptive attacks [53].

Generative classifiers. Generative classifiers, like naive Bayes [35], predict the class probabilities $p(y|\mathbf{x})$ for a given input $\mathbf{x}$ by modeling the data likelihood $p(\mathbf{x}|y)$ using generative models. Compared with discriminative classifiers, generative classifiers are often more robust and well-calibrated [31, 35, 39, 43]. Modern generative models like diffusion models [23], energy-based models [29] can also be used as generative classifiers. SBGC [62] utilizes a score-based model to calculate the log-likelihood $\log p(\mathbf{x}|y)$ by integration and then calculates $p(y|\mathbf{x})$ via Bayes' theorem. HybViT [59] directly learns the joint likelihood $\log p(\mathbf{x}, y) = \log p(\mathbf{x}) + \log p(y|\mathbf{x})$ by training a diffusion model to learn $\log p(\mathbf{x})$ and a standard classifier to model $\log p(y|\mathbf{x})$ at training time, and direct predicts $p(y|\mathbf{x})$ at test time. JEM [20] utilizes the energy-based model to predict joint likelihood $\log p(\mathbf{x}, y)$ and Bayes' theorem to get $p(y|\mathbf{x})$. We also compare with these generative classifiers in the experiments. Two concurrent works [7, 30] also convert diffusion models to generative classifiers in a similar way to ours, but they mainly focus on zero-shot classification while do not consider the adversarial robustness.

Diffusion models for adversarial robustness. As a powerful family of generative models [11, 23], diffusion models have been introduced to further boost adversarial robustness. DiffPure [37] utilizes diffusion models to purify adversarial perturbations by first adding Gaussian noises to input images and then denoising the images. Diffusion models can also help to improve the certified robustness with randomized smoothing [6, 58]. Besides, using data generated by diffusion models can significantly improve the performance of adversarial training [40, 55]. However, DiffPure is vulnerable to stronger adaptive attacks (as shown in Table 1), while adversarial training does not generalize well across different threat models (as shown in Table 2). A potential reason of their problems is that they still focus on discriminative classifiers, which do not capture the underlying structure of data distribution. As diffusion models have more accurate score estimation in the whole data space, we aim to explore whether a diffusion model itself can be leveraged to build a robust classifier.

3 Methodology

In this section, we present our **Robust Diffusion Classifier (RDC)**, a robust (generative) classifier constructed from a pre-trained diffusion model. We first provide an overview of diffusion models in Sec. 3.1, then present how to convert a (class-conditional) diffusion model into a classifier in Sec. 3.2 with a robustness analysis considering the optimal setting in Sec. 3.3, and finally detail the likelihood maximization and variance reduction techniques to further improve the robustness and efficiency in Sec. 3.4 and Sec. 3.5, respectively. Fig. 1 illustrates our approach.

3.1 Preliminary: diffusion models

We briefly review discrete-time diffusion models [23, 45]. Given a real data distribution $\mathbf{x}_0 := \mathbf{x} \sim q(\mathbf{x})$, the forward diffusion process gradually adds Gaussian noise to the data to obtain a sequence of noisy samples $\{\mathbf{x}_t\}_{t=1}^T$ according to a scaling schedule $\{\alpha_t\}_{t=1}^T$ and a noise schedule $\{\sigma_t\}_{t=1}^T$ as

$$q(\mathbf{x}_t|\mathbf{x}_0) = \mathcal{N}(\mathbf{x}_t; \sqrt{\alpha_t}\mathbf{x}_0, \sigma_t^2\mathbf{I}). \tag{1}$$

Assume that the signal-to-noise ratio $\text{SNR}(t) = \alpha_t/\sigma_t^2$ is strictly monotonically decreasing in time, the sample $\mathbf{x}_t$ is increasingly noisy during the forward process. The scaling and noise schedules are prescribed such that $\mathbf{x}_T$ is nearly an isotropic Gaussian distribution.

To generate images, we need to reverse the diffusion process. It is defined as a Markov chain with learned Gaussian distributions as

$$p_\theta(\mathbf{x}_{0:T}) = p(\mathbf{x}_T)\prod_{t=1}^{T} p_\theta(\mathbf{x}_{t-1}|\mathbf{x}_t), \quad p_\theta(\mathbf{x}_{t-1}|\mathbf{x}_t) = \mathcal{N}(\mathbf{x}_{t-1}; \boldsymbol{\mu}_\theta(\mathbf{x}_t, t), \tilde{\sigma}_t^2\mathbf{I}), \tag{2}$$

where $p(\mathbf{x}_T) = \mathcal{N}(\mathbf{x}_T; \mathbf{0}, \mathbf{I})$ is a prior distribution. Instead of directly parameterizing $\boldsymbol{\mu}_\theta$ via neural networks, it is a common practice [23, 25, 49] to rewrite $\boldsymbol{\mu}_\theta$ as

$$\boldsymbol{\mu}_\theta(\mathbf{x}_t, t) = \sqrt{\frac{\alpha_{t-1}}{\alpha_t}}\left(\mathbf{x}_t - \sqrt{\frac{\sigma_t}{1-\alpha_t}}\boldsymbol{\epsilon}_\theta(\mathbf{x}_t, t)\right), \tag{3}$$

and learn the time-conditioned noise prediction network $\boldsymbol{\epsilon}_\theta(\mathbf{x}_t, t)$. It can be learned by optimizing the variational lower bound on log-likelihood as

$$\begin{aligned}\log p_\theta(\mathbf{x}) &\geq \mathbb{E}_q[-D_{\mathrm{KL}}(q(\mathbf{x}_T|\mathbf{x}_0)\|p(\mathbf{x}_T)) - \sum_{t>1} D_{\mathrm{KL}}(q(\mathbf{x}_{t-1}|\mathbf{x}_t, \mathbf{x}_0)\|p_\theta(\mathbf{x}_{t-1}|\mathbf{x}_t)) + \log p_\theta(\mathbf{x}_0|\mathbf{x}_1)] \\ &= -\mathbb{E}_{\boldsymbol{\epsilon},t}\left[w_t\|\boldsymbol{\epsilon}_\theta(\mathbf{x}_t, t) - \boldsymbol{\epsilon}\|_2^2\right] + C_1,\end{aligned} \tag{4}$$

where $\mathbb{E}_{\boldsymbol{\epsilon},t}[w_t\|\boldsymbol{\epsilon}_\theta(\mathbf{x}_t, t) - \boldsymbol{\epsilon}\|_2^2]$ is called *diffusion loss* [25], $\boldsymbol{\epsilon}$ follows the standard Gaussian distribution $\mathcal{N}(\mathbf{0}, \mathbf{I})$, $\mathbf{x}_t = \sqrt{\alpha_0}\mathbf{x}_0 + \sigma_t\boldsymbol{\epsilon}$ given by Eq. (1), C_1 is typically small and can be dropped [23, 49], and $w_t = \frac{\sigma_t\alpha_{t-1}}{2\tilde{\sigma}_t^2(1-\alpha_t)\alpha_t}$. In practice, we set $w_t = 1$ for convenience and good performance as in [23].

For conditional generation [22], the conditional diffusion model $p_\theta(\mathbf{x}|y)$ can be parameterized by $\boldsymbol{\epsilon}_\theta(\mathbf{x}_t, t, y)$, while the unconditional model $p_\theta(\mathbf{x})$ can be seen as a special case with a null input as $\boldsymbol{\epsilon}_\theta(\mathbf{x}_t, t) = \boldsymbol{\epsilon}_\theta(\mathbf{x}_t, t, y = \varnothing)$. A similar lower bound on the conditional log-likelihood is

$$\log p_\theta(\mathbf{x}|y) \geq -\mathbb{E}_{\boldsymbol{\epsilon},t}\left[w_t\|\boldsymbol{\epsilon}_\theta(\mathbf{x}_t, t, y) - \boldsymbol{\epsilon}\|_2^2\right] + C, \tag{5}$$

where C is another small constant that is negligible.

3.2 Diffusion model for classification

Given an input $\mathbf{x}$, a classifier computes the probability $p_\theta(y|\mathbf{x})$ for all classes $y \in \{1, 2, .., K\}$ with K being the number of classes and outputs the most probable class as $\tilde{y} = \arg\max_y p_\theta(y|\mathbf{x})$. Popular discriminative approaches train Convolutional Neural Networks [21, 27] or Vision Transformers [15, 33] to directly learn the conditional probability $p_\theta(y|\mathbf{x})$. However, they cannot predict accurately for adversarial example $\mathbf{x}^*$ that is close to the real example $\mathbf{x}$ under the ℓ_p norm as $\|\mathbf{x}^* - \mathbf{x}\|_p \leq \epsilon_p$, since it is hard to control how inputs are classified outside the training distribution [43].

On the other hand, diffusion models are trained to provide accurate density estimation over the entire data space [23, 47, 49]. By transforming a diffusion model into a generative classifier through Bayes' theorem as $p_\theta(y|\mathbf{x}) \propto p_\theta(\mathbf{x}|y)p(y)$, we hypothesize that the classifier can also give a more accurate conditional probability $p_\theta(y|\mathbf{x})$ in the data space, leading to better adversarial robustness. In this paper, we assume a uniform prior $p(y) = \frac{1}{k}$ for simplicity, which is common for most of the datasets [26, 41]. We show how to compute the conditional probability $p_\theta(y|\mathbf{x})$ via a diffusion model in the following theorem.

Theorem 3.1. *(Proof in Appendix A) Let $d(\mathbf{x}, y, \theta) = \log p_\theta(\mathbf{x}|y) + \mathbb{E}_{\boldsymbol{\epsilon},t}[w_t\|\boldsymbol{\epsilon}_\theta(\mathbf{x}_t, t, y) - \boldsymbol{\epsilon}\|_2^2]$ denote the gap between the log-likelihood and the diffusion loss. Assume that y is uniformly distributed as $p(y) = \frac{1}{K}$ and $\forall y$, $d(\mathbf{x}, y, \theta) \to 0$. Then the conditional probability $p_\theta(y|\mathbf{x})$ can be approximated by*

$$p_\theta(y|\mathbf{x}) = \frac{\exp(-\mathbb{E}_{\boldsymbol{\epsilon},t}[w_t\|\boldsymbol{\epsilon}_\theta(\mathbf{x}_t, t, y) - \boldsymbol{\epsilon}\|_2^2])}{\sum_{\hat{y}}\exp(-\mathbb{E}_{\boldsymbol{\epsilon},t}[w_t\|\boldsymbol{\epsilon}_\theta(\mathbf{x}_t, t, \hat{y}) - \boldsymbol{\epsilon}\|_2^2])}. \tag{6}$$

In Theorem 3.1, we approximate the conditional log-likelihood with the (negative) diffusion loss, which holds true when the gap $d(\mathbf{x}, y, \theta)$ is 0. In practice, although there is inevitably a gap between the log-likelihood and the diffusion loss, we show that the approximation works well in experiments. Eq. (6) requires calculating the noise prediction error over the expectation of random noise $\boldsymbol{\epsilon}$ and timestep t, which is efficiently estimated with the variance reduction technique introduced in Sec. 3.5. Besides, our method is also applicable when the prior $p(y)$ is not uniform if we add the logit of class y by $\log p(y)$, where $p(y)$ can be estimated from the training data. Below, we provide an analysis on the adversarial robustness of the diffusion classifier in Eq. (6) under the optimal setting.

3.3 Robustness analysis under the optimal setting

To provide a deeper understanding of the robustness of our diffusion classifier, we first derive the optimal solution of the diffusion model, as shown in the following theorem.

Theorem 3.2. *(Proof in Appendix B.1) Let D denote a set of examples and $D_y \subset D$ denote a subset of examples whose ground-truth label is y. The optimal diffusion model $\boldsymbol{\epsilon}_{\theta^*_D}(\mathbf{x}_t, t, y)$ on the set D is*

$$\boldsymbol{\epsilon}_{\theta^*_D}(\mathbf{x}_t, t, y) = \sum_{\mathbf{x}^{(i)} \in D_y} \frac{1}{\sigma_t}(\mathbf{x}_t - \sqrt{\alpha_t}\mathbf{x}^{(i)}) \cdot \mathrm{softmax}\left(-\frac{1}{2\sigma_t^2}\|\mathbf{x}_t - \sqrt{\alpha_t}\mathbf{x}^{(i)}\|_2^2\right), \tag{7}$$

where $\mathrm{softmax}(\cdot)$ *denotes the softmax function.*

Given the optimal diffusion model in Eq. (7), we can easily obtain the optimal diffusion classifier by substituting the solution in Eq. (7) into Eq. (6).

Corollary 3.3. *(Proof in Appendix B.2) The conditional probability $p_{\theta^*_D}(y|\mathbf{x})$ given the optimal diffusion model $\boldsymbol{\epsilon}_{\theta^*_D}(\mathbf{x}_t, t, y)$ is*

$$p_{\theta^*_D}(y|\mathbf{x}) = \mathrm{softmax}\left(f_{\theta^*_D}(\mathbf{x})_y\right), \; f_{\theta^*_D}(\mathbf{x})_y = -\mathbb{E}_{\boldsymbol{\epsilon},t}\left[\frac{\alpha_t}{\sigma_t^2}\Big\| \sum_{\mathbf{x}^{(i)} \in D_y} s(\mathbf{x}, \mathbf{x}^{(i)}, \boldsymbol{\epsilon}, t)(\mathbf{x} - \mathbf{x}^{(i)})\Big\|_2^2\right],$$

where

$$s(\mathbf{x}, \mathbf{x}^{(i)}, \boldsymbol{\epsilon}, t) = \mathrm{softmax}\left(-\frac{1}{2\sigma_t^2}\|\sqrt{\alpha_t}\mathbf{x} + \sigma_t\boldsymbol{\epsilon} - \sqrt{\alpha_t}\mathbf{x}^{(i)}\|_2^2\right).$$

Remark. Intuitively, the optimal diffusion classifier utilizes the ℓ_2 norm of the weighted average difference between the input example $\mathbf{x}$ and the real examples $\mathbf{x}^{(i)}$ of class y to calculate the logit for $\mathbf{x}$. The classifier will predict a label $\tilde{y}$ for an input $\mathbf{x}$ if it lies more closely to real examples belonging to $D_{\tilde{y}}$. Moreover, the ℓ_2 norm is averaged over t with weight $\frac{\alpha_t}{\sigma_t^2}$. As $\frac{\alpha_t}{\sigma_t^2}$ is monotonically decreasing w.r.t. t, the classifier gives small weights for noisy examples and large weights for clean examples, which is reasonable since the noisy examples do not play an important role in classification.

Empirically, we evaluate the robust accuracy of the optimal diffusion classifier under the ℓ_∞ norm with $\epsilon_\infty = 8/255$ and the ℓ_2 norm with $\epsilon_2 = 0.5$. We find that the optimal diffusion classifier achieves 100% robust accuracy in both cases, validating our hypothesize that accurate density estimation of diffusion models facilitates robust classification. However, the diffusion models are not optimal in practice. Our trained diffusion classifier can only achieve 35.94% and 76.95% robust accuracy under the ℓ_∞ and ℓ_2 threats, as shown in Table 1. Despite the non-trivial performance without adversarial training, it still lags behind the state-of-the-art. To figure out the problem, we find that the diffusion loss $\mathbb{E}_{\boldsymbol{\epsilon},t}[w_t\|\boldsymbol{\epsilon}_\theta(\mathbf{x}_t, t, y) - \boldsymbol{\epsilon}\|_2^2$ is very large for some adversarial example with the ground-truth class. This is caused by either the inaccurate density estimation of $p_\theta(\mathbf{x}|y)$ of the diffusion model or the large gap between the log-likelihood and the diffusion loss violating $d(\mathbf{x}, y, \theta) \to 0$. Developing a better conditional diffusion model can help to address this issue, but we leave this to future work. In the following section, we propose an optimization-based algorithm as an alternative strategy to solve the problem with off-the-shelf diffusion models.

3.4 Likelihood maximization

To address the aforementioned problem, a straightforward approach is to minimize the diffusion loss $\mathbb{E}_{\boldsymbol{\epsilon},t}[w_t\|\boldsymbol{\epsilon}_\theta(\mathbf{x}_t, t, y) - \boldsymbol{\epsilon}\|_2^2]$ w.r.t. $\mathbf{x}$ such that the input can escape from the region that the diffusion model cannot provide an accurate density estimation or the gap between the likelihood and diffusion loss $d(\mathbf{x}, y, \theta)$ is large. However, we do not know the ground-truth label of $\mathbf{x}$, making the optimization infeasible. As an alternative strategy, we propose to minimize the unconditional diffusion loss as

$$\min_{\hat{\mathbf{x}}} \mathbb{E}_{\boldsymbol{\epsilon},t}[w_t\|\boldsymbol{\epsilon}_\theta(\hat{\mathbf{x}}_t, t) - \boldsymbol{\epsilon}\|_2^2], \quad \text{s.t. } \|\hat{\mathbf{x}} - \mathbf{x}\|_\infty \leq \eta, \tag{8}$$

where we restrict the ℓ_∞ norm between the optimized input $\hat{\mathbf{x}}$ and the original input $\mathbf{x}$ to be smaller than η, in order to avoid optimizing $\hat{\mathbf{x}}$ into the region of other classes. As Eq. (8) actually maximizes the lower bound of the log-likelihood in Eq. (4), we call this approach **Likelihood Maximization**.

Algorithm 1 Robust Diffusion Classifier (RDC)

Require: A pre-trained diffusion model $\boldsymbol{\epsilon}_\theta$, input image $\mathbf{x}$, optimization budget η, step size γ, optimization steps N, momentum decay factor μ.

Initialize: $\mathbf{m} = 0, \hat{\mathbf{x}} = \mathbf{x}$;
for $n = 0$ **to** $N - 1$ **do**
  Calculate $\mathbf{g} = \nabla_{\mathbf{x}} \mathbb{E}_{\boldsymbol{\epsilon},t}[w_t \|\boldsymbol{\epsilon}_\theta(\hat{\mathbf{x}}_t, t) - \boldsymbol{\epsilon}\|_2^2]$ via Eq. (9);
  Update momentum $\mathbf{m} = \mu \cdot \mathbf{m} - \frac{\mathbf{g}}{\|\mathbf{g}\|_1}$;
  Update $\hat{\mathbf{x}}$ by $\hat{\mathbf{x}} = \text{clip}_{\mathbf{x},\eta}(\hat{\mathbf{x}} + \gamma \cdot \text{sign}(\mathbf{m}))$;
end for
for $y = 1$ **to** K **do**
  Calculate $\mathbb{E}_{\boldsymbol{\epsilon},t}[w_t \|\boldsymbol{\epsilon}_\theta(\hat{\mathbf{x}}_t, t, y) - \boldsymbol{\epsilon}\|_2^2]$ via Eq. (9);
end for
Calculate $p_\theta(y|\mathbf{x})$ by Eq. (6);
Return: $\tilde{y} = \arg\max_y p_\theta(y|\mathbf{x})$.

By solving Eq. (8), the optimized input $\hat{\mathbf{x}}$ will have a higher log-likelihood [19], indicating that $\hat{\mathbf{x}}$ is closer to real data. This method can also be understood as input purification. Besides, because the adversarial example usually lies in the vicinity of its corresponding real example of the ground-truth class y, moving along the direction towards higher $\log p(\mathbf{x})$ will probably lead to higher $\log p(\mathbf{x}|y)$. Therefore, the optimized input $\hat{\mathbf{x}}$ could be more accurately classified by the diffusion classifier. Note that the likelihood maximization is different from other diffusion-based purification approaches [3, 37, 54], as they aim to remove the adversarial noises but we aim to optimize the data towards high log-likelihood to be easily classified by our diffusion classifier. We solve Eq. (8) with the momentum optimizer [12] to stabilize the gradient direction and avoid non-desirable local optima.

3.5 Variance reduction

To estimate the diffusion loss in Eq. (6) and Eq. (8) over the expectation of $\boldsymbol{\epsilon}$ and t, a common practice is to adopt the Monte Carlo sampling, which will lead to a high variance with few samples or high time complexity with many samples. To reduce the variance with affordable computational cost, we directly compute the expectation over t instead of sampling t as

$$\mathbb{E}_{\boldsymbol{\epsilon},t}[w_t \|\boldsymbol{\epsilon}_\theta(\mathbf{x}_t, t, y) - \boldsymbol{\epsilon}\|_2^2] = \frac{1}{T} \sum_{t=1}^{T} \mathbb{E}_{\boldsymbol{\epsilon}}[w_t \|\boldsymbol{\epsilon}_\theta(\mathbf{x}_t, t, y) - \boldsymbol{\epsilon}\|_2^2]. \tag{9}$$

Eq. (9) requires to calculate the noise prediction error for all timesteps. For $\boldsymbol{\epsilon}$, we still adopt Monte Carlo sampling, but we show that sampling only one $\boldsymbol{\epsilon}$ is sufficient to achieve good performance. Thus the diffusion classifier in Eq. (6) needs $K \times T$ forward passes of the diffusion model, which is more computationally expensive than discriminative classifiers, as a major limitation of our method originated from diffusion models [2]. We can further reduce the number of timesteps by systematic sampling that selects the timesteps at a uniform interval. Although it does not lead to an obvious drop in clean accuracy, it will significantly affect robust accuracy as shown in Sec. 4.5, because the objective is no longer strongly correlated with log-likelihood after reducing the number of timesteps. Given the above techniques, the overall algorithm of RDC is outlined in Algorithm 1.

4 Experiments

In this section, we first provide the experimental settings in Sec. 4.1. We then show the effectiveness of our method compared with the state-of-the-art methods in Sec. 4.2 and the generalizability across different threat models in Sec. 4.3. We provide thorough analysis to examine gradient obfuscation in Sec. 4.4 and conduct various ablation studies in Sec. 4.5.

4.1 Experimental settings

Datasets and training details. We conduct experiments on the CIFAR-10 dataset [26]. For the conditional diffusion model, we train it on the CIFAR-10 training set using the NCSN++ architecture [49] and classifier-free guidance [22]. For robustness evaluation, we randomly select 512 images from the CIFAR-10 test set due to the high computational cost of the attack algorithms, following [37].

Table 1: Clean accuracy (%) and robust accuracy (%) of different methods against AutoAttack under the ℓ_∞ norm with $\epsilon_\infty = 8/255$ and the ℓ_2 norm with $\epsilon_2 = 0.5$. RDC outperforms the best adversarial training method AT-EDM [55] by **+2.34%** under the ℓ_∞ norm.

	Architecture	ℓ_∞ norm		ℓ_2 norm	
		Clean Acc	Robust Acc	Clean Acc	Robust Acc
AT-DDPM [40]	WRN70-16	88.87	63.28	93.16	81.05
AT-EDM [55]	WRN70-16	93.36	70.90	95.90	**84.77**
DiffPure [37]	UNet+WRN70-16	90.97	53.52	92.68	75.98
SBGC [62]	UNet	95.04	0.00	95.04	0.00
HybViT [59]	ViT	95.90	0.00	95.90	0.00
JEM [20]	WRN28-10	92.90	8.20	92.90	26.37
DC (ours)	UNet	93.55	35.94	93.55	76.95
RDC (ours)	UNet	93.16	**73.24**	93.16	**80.27**

Hyperparameters. In likelihood maximization, we set the optimization steps $N = 10$, momentum decay factor $\mu = 1$, optimization budget $\eta = 8/255$ (see Sec. 4.5 for an ablation study), step size $\gamma = \eta/N$. For each timestep, we only sample one $\boldsymbol{\epsilon}$ to estimate $\mathbb{E}_{\boldsymbol{\epsilon}}[w_t \|\boldsymbol{\epsilon}_\theta(\mathbf{x}_t, t, y) - \boldsymbol{\epsilon}\|_2^2]$.

Robustness evaluation. Following [37], we evaluate the clean accuracy and robust accuracy of our method by AutoAttack [9] under both ℓ_∞ norm of $\epsilon_\infty = 8/255$ and ℓ_2 norm of $\epsilon_2 = 0.5$. To demonstrate the generalization ability towards unseen threat models, we also utilize StAdv [57] with 100 steps under the bound of 0.05 to evaluate our method. As computing the gradient through the likelihood maximization method requires to calculate the second-order derivative, we use BPDA [1] as the default adaptive attack, which approximates the gradient with an identity mapping. We conduct more comprehensive evaluations of gradient obfuscation under other adaptive attacks in Sec. 4.4, where we show that BPDA is as strong as computing the exact gradient.

4.2 Comparison with the state-of-the-art

We compare our method with the state-of-the-art defense methods on RobustBench [10], including adversarial training with DDPM generated data (AT-DDPM) [40] (rank 2), adversarial training with EDM generated data (AT-EDM) [55] (rank 1), and DiffPure [37]. These models adopt the WRN70-16 architecture [60]. We also compare our method with other generative classifiers, including SBGC [62], HybViT [59], and JEM [20]. Notably, robust accuracy of most baselines does not change much on our selected subset, compared with the results on RobustBench [10].

DiffPure incurs significant memory usage and introduces substantial randomness, posing challenges for robustness evaluation. Their proposed adjoint method [37] is insufficient to measure the model robustness. To mitigate this issue, we employ gradient checkpoints to obtain an accurate gradient computation and leverage Expectation Over Time (EOT) to reduce the impact of randomness during optimization. Rather than using the 640 times EOT recommended in Fig. 2(c), we adopt PGD-80 [34] with 10 times EOT and a large step size $1/255$ to efficiently evaluate DiffPure.

Table 1 shows the robustness of Diffusion Classifier (DC, without likelihood maximization) and Robust Diffusion Classifier (RDC) compared with baselines under the ℓ_∞ and ℓ_2 norm threat models. We can see that the robustness of DC outperforms all previous generative classifiers by a large margin. Specifically, DC improves the robust accuracy over JEM by +27.74% under the ℓ_∞ norm and +50.58% under the ℓ_2 norm. RDC can further improve the performance over DC, which achieves 73.27% and 80.27% robust accuracy under the two settings. Notably, RDC outperforms the previous state-of-the-art model AT-EDM [55] by +2.34% under the ℓ_∞ norm. Although RDC does not outperform the best adversarial training models under the ℓ_2 norm because likelihood maximization adopts the ℓ_∞ norm in Eq. (8), it could be solved by adjusting the optimization constraint (See Appendix C for details). In the following section, we demonstrate that using the same optimization constraint allows our method to be threat model agnostic, resulting in strong generalization abilities against unseen threat models.

4.3 Defense against unseen threats

Adversarial training methods often suffer from poor generalization across different threat models, while DiffPure requires adjusting purification noise scales for different threat models, which limits

Table 2: Clean accuracy (%) and robust accuracy (%) of different methods against unseen threats.

Method	Clean Acc	Robust Acc			
		ℓ_∞ norm	ℓ_2 norm	StAdv	Avg
AT-DDPM-ℓ_∞ [40]	88.87	63.28	64.65	4.88	44.27
AT-DDPM-ℓ_2 [40]	93.16	49.41	81.05	5.27	45.24
AT-EDM-ℓ_∞ [55]	93.36	70.90	69.73	2.93	47.85
AT-EDM-ℓ_2 [55]	95.90	53.32	84.77	5.08	47.72
PAT-self [28]	75.59	47.07	64.06	39.65	50.26
DiffPure ($t^* = 0.125$) [37]	87.50	53.12	75.59	12.89	47.20
DC (ours)	93.55	35.94	76.95	93.55	**68.81**
RDC (ours)	93.16	73.24	80.27	91.41	**81.64**

their applicability in real-world scenarios where the threat models are unknown. In contrast, our proposed methods are agnostic to specific threat models. To demonstrates the strong generalization ability of our methods across different threat models, we evaluate the generalization performance of our proposed method by testing against different threats, including ℓ_∞, ℓ_2, and StAdv.

Table 2 presents the results, which shows that the average robustness of our methods (DC and RDC) surpass the baselines by more than 30%. Specifically, our model outperforms ℓ_∞ adversarial training models by +10.54% under the ℓ_2 attack and ℓ_2 adversarial training models by +19.92% under the ℓ_∞ attack. Impressively, DC and RDC achieve 93.55% and 91.41% robustness under StAdv, surpassing adversarial training models by more than 86.14%. These results indicate the strong generalization ability of our method and its potential to be applied in real-world scenarios under unknown threats.

4.4 Evaluation of gradient obfuscation

Diffusion Classifier can be directly evaluate by AutoAttack [9]. However, Robust Diffusion Classifier could not be directly evaluated by AutoAttack due to the indifferentiable likelihood maximization. To demonstrate the effectiveness of BPDA adaptive attack, we conduct the following experiments.

Exact gradient attack. To directly evaluate the robustness of RDC, we utilize gradient checkpoint and create a computational graph during backpropagation to obtain exact gradients. However, we could only evaluate RDC when $N = 1$ due to the large memory cost. As shown in Table 3, our RDC with $N = 1$ achieves 69.53% robust accuracy under the exact gradient attack, about 0.39% lower than BPDA. This result suggests that BPDA suffices for evaluating RDC.

Table 3: Robust accuracy (%) of RDC under different adaptive attacks. BPDA ($N = 10$) and Lagrange ($N = 10$) are adaptive attacks for RDC with 10 steps of likelihood maximization, while Exact Gradient ($N = 1$) and BPDA ($N = 1$) are adaptive attacks for RDC with 1 step.

Attack	Robust Acc
BPDA ($N = 10$)	73.24
Lagrange ($N = 10$)	77.54
Exact Gradient ($N = 1$)	69.53
BPDA ($N = 1$)	69.92

Lagrange attack. RDC optimizes the unconditional diffusion loss before feeding the inputs into DC. If our adversarial examples already have a small unconditional diffusion loss or a large $\log p(\mathbf{x})$, it may not be interrupted during likelihood maximization. Therefore, to produce adversarial examples with a small diffusion loss, we set our loss function as follows:

$$\text{Lagrange}(\mathbf{x}, y, \boldsymbol{\epsilon}_\theta) = \log p_\theta(y|\mathbf{x}) + l \cdot \mathbb{E}_{\boldsymbol{\epsilon},t}[w_t \|\boldsymbol{\epsilon}_\theta(\mathbf{x}_t, t) - \boldsymbol{\epsilon}\|_2^2], \tag{10}$$

where $p_\theta(y|\mathbf{x})$ is given by Eq. (6), and the first term is the (negative) cross-entropy loss to induce misclassification. For an input, we craft adversarial examples using three different weights, $l = 0, 1, 10$. If one of these three loss functions successfully generate an adversarial example, we count it as a successful attack. As shown in Table 3, this adaptive attack is no more effective than BPDA.

Gradient randomness. To quantify the randomness of our methods, we compute the gradients of each model w.r.t. the input ten times and compute the pairwise cosine similarity between the gradients. We then average these cosine similarities across 100 images. To capture the randomness when using EOT, we treat the gradients obtained after applying EOT as a single time and repeat the same process to compute their cosine similarity. As shown in Fig. 2(c), the gradients of our methods exhibit low randomness, while DiffPure is more than 640 times as random as DC, RDC-1, and about

320 times as random as RDC-BPDA-10. Thus, the robustness of our methods is not primarily due to the stochasticity of gradients.

Diffusion likelihood maximizer. We also combine likelihood maximization with the traditional classifier WRN70-16 [60] and evaluate this approach alongside our RDC on 100 randomly selected images from CIFAR-10. Under the BPDA attack, the WRN70-16 with likelihood maximization achieves only 2% robustness, while our RDC achieves 76% robustness. This is because the likelihood maximization moves the inputs towards high log-likelihood region estimated by diffusion models, instead of traditional classifiers, thus it is only effective when combining with diffusion classifiers. This result also suggests that BPDA attack is effective against optimization-based defenses, and the robustness of RDC is not attributed to the indifferentiability of likelihood maximization.

4.5 Ablation studies

In this section, we perform ablation studies of several hyperparameters in our algorithm with the first 100 examples in the CIFAR-10 test set. All the experiments are done under AutoAttack with BPDA of ℓ_∞ bounded perturbations with $\epsilon_\infty = 8/255$.

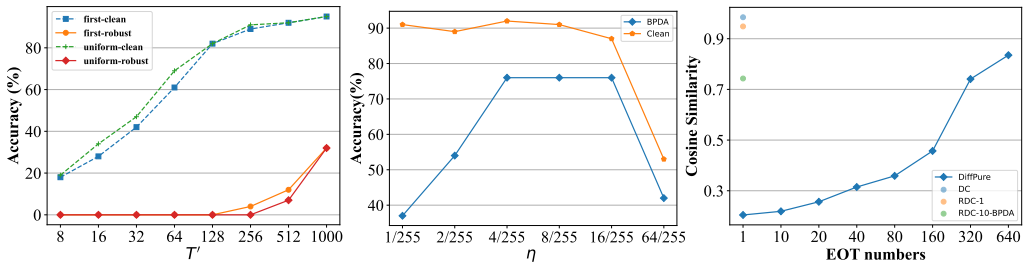

(a) T' (b) ablation of η (c) Randomness

Figure 2: (a-b): Impact of T' and η in our method on standard accuracy and robust accuracy against our BPDA adaptive attack. (c): Randomness of different methods, where RDC-1 denotes RDC with $N = 1$ using the exact gradient, and RDC-10-BPDA denotes RDC with $N = 10$ using BPDA.

Optimization budget η. To find the best optimization budget η, we test the robust accuracy of different optimization budgets. As shown in Fig. 2(b), the robust accuracy first increases and then decreases as η becomes larger. When η is small, we could not move $\mathbf{x}$ out of the adversarial region. However, when η is too large, we may optimize $\mathbf{x}$ into an image of another class. Therefore, we should choose an appropriate η. In this work, we set $\eta = 8/255$.

Momentum optimizer. We then study the optimization algorithm for likelihood maximization in Eq. (8). Optimizing without momentum results in 69% robustness, which is approximately 7% lower than that with momentum. This suggests that a better optimization algorithm could decrease the unconditional diffusion loss more effectively, thus improving the robustness. Using more advanced optimization algorithms for likelihood maximization may lead to even greater robustness, and we leave this to future works.

Sampling timesteps. We also try to further reduce the number of sampling timesteps. One way is to only calculate the diffusion loss of the first T' timesteps $\{i\}_{i=1}^{T'}$ (named "first"). Inspired by [46], another way is to use systematic sampling, where we use timesteps $\{iT/T'\}_{i=1}^{T'}$ (named "uniform"). The results are shown in Fig. 2(a). Both methods achieve similar results on clean accuracy and robust accuracy. Although a significant reduction of T' does not lead to an obvious drop in clean accuracy, it will significantly affect robust accuracy due to the reason discussed in Sec. 3.5.

Sampling steps for $\boldsymbol{\epsilon}$. We also attempt to improve the accuracy of estimation of $\mathbb{E}_{\boldsymbol{\epsilon}}[w_t \|\boldsymbol{\epsilon}_\theta(\mathbf{x}_t, t, y) - \boldsymbol{\epsilon}\|_2^2]$ in Eq. (9) by sampling $\boldsymbol{\epsilon}$ multiple times or keeping $\boldsymbol{\epsilon}$ the same for different timesteps or different classes. However, these increase neither robustness nor accuracy because we have already computed T times for the expectation over t. From another perspective, the cosine similarity of the gradients is about 98.48%, suggesting that additional sampling of $\boldsymbol{\epsilon}$ or using the same $\boldsymbol{\epsilon}$ for different timesteps or classes is unnecessary.

5 Conclusion

In this paper, we propose a novel defense method called Robust Diffusion Classifier (RDC), which leverages an off-the-shelf diffusion model to directly classify input images by predicting data likelihood by diffusion model and calculating class probabilities through Bayes' theorem. We theoretically analyze the robustness of our diffusion classifier, propose to maximize the log-likelihood before feeding the input images into the diffusion classifier, and greatly improve the robustness. To demonstrate the performance of our method, we evaluate our method with strong adaptive attacks and conduct extensive experiments. Our method achieves state-of-the-art robustness against these strong adaptive attacks and generalizes well to unseen threat models.

Despite the great improvement, our methods still need to be further improved. First, the high time complexity for calculating the diffusion loss makes our methods hard to apply in real scenarios, and this could be solved by applying more efficient diffusion models [2, 46, 50]. Besides, the conditional diffusion model in this paper is directly adopted from existing works, and training a better conditional diffusion model could further improve the performance. We hope our work could give an encouraging step toward designing robust classifiers using generative models.

References

[1] Anish Athalye, Nicholas Carlini, and David Wagner. Obfuscated gradients give a false sense of security: Circumventing defenses to adversarial examples. In *International Conference on Machine Learning*, pages 274–283, 2018.

[2] Fan Bao, Chongxuan Li, Jun Zhu, and Bo Zhang. Analytic-dpm: an analytic estimate of the optimal reverse variance in diffusion probabilistic models. In *International Conference on Learning Representations*, 2022.

[3] Tsachi Blau, Roy Ganz, Bahjat Kawar, Alex Bronstein, and Michael Elad. Threat model-agnostic adversarial defense using diffusion models. *arXiv preprint arXiv:2207.08089*, 2022.

[4] Yulong Cao, Ningfei Wang, Chaowei Xiao, Dawei Yang, Jin Fang, Ruigang Yang, Qi Alfred Chen, Mingyan Liu, and Bo Li. Invisible for both camera and lidar: Security of multi-sensor fusion based perception in autonomous driving under physical-world attacks. In *2021 IEEE Symposium on Security and Privacy*, pages 176–194, 2021.

[5] Nicholas Carlini and David Wagner. Towards evaluating the robustness of neural networks. In *IEEE Symposium on Security and Privacy*, pages 39–57, 2017.

[6] Nicholas Carlini, Florian Tramer, Krishnamurthy Dj Dvijotham, Leslie Rice, Mingjie Sun, and J Zico Kolter. (certified!!) adversarial robustness for free! In *International Conference on Learning Representations*, 2023.

[7] Kevin Clark and Priyank Jaini. Text-to-image diffusion models are zero-shot classifiers. *arXiv preprint arXiv:2303.15233*, 2023.

[8] Jeremy Cohen, Elan Rosenfeld, and Zico Kolter. Certified adversarial robustness via randomized smoothing. In *International Conference on Machine Learning*, pages 1310–1320, 2019.

[9] Francesco Croce and Matthias Hein. Reliable evaluation of adversarial robustness with an ensemble of diverse parameter-free attacks. In *International Conference on Machine Learning*, pages 2206–2216, 2020.

[10] Francesco Croce, Maksym Andriushchenko, Vikash Sehwag, Edoardo Debenedetti, Nicolas Flammarion, Mung Chiang, Prateek Mittal, and Matthias Hein. Robustbench: a standardized adversarial robustness benchmark. In *Thirty-fifth Conference on Neural Information Processing Systems Datasets and Benchmarks Track*, 2020.

[11] Prafulla Dhariwal and Alexander Nichol. Diffusion models beat gans on image synthesis. *Advances in Neural Information Processing Systems*, pages 8780–8794, 2021.

[12] Yinpeng Dong, Fangzhou Liao, Tianyu Pang, Hang Su, Jun Zhu, Xiaolin Hu, and Jianguo Li. Boosting adversarial attacks with momentum. In *Proceedings of the IEEE/CVF Conference on Computer Vision and Pattern Recognition*, pages 9185–9193, 2018.

[13] Yinpeng Dong, Tianyu Pang, Hang Su, and Jun Zhu. Evading defenses to transferable adversarial examples by translation-invariant attacks. In *Proceedings of the IEEE/CVF Conference on Computer Vision and Pattern Recognition*, pages 4312–4321, 2019.

[14] Yinpeng Dong, Hang Su, Baoyuan Wu, Zhifeng Li, Wei Liu, Tong Zhang, and Jun Zhu. Efficient decision-based black-box adversarial attacks on face recognition. In *Proceedings of the IEEE/CVF Conference on Computer Vision and Pattern Recognition*, pages 7714–7722, 2019.

[15] Alexey Dosovitskiy, Lucas Beyer, Alexander Kolesnikov, Dirk Weissenborn, Xiaohua Zhai, Thomas Unterthiner, Mostafa Dehghani, Matthias Minderer, Georg Heigold, Sylvain Gelly, et al. An image is worth 16x16 words: Transformers for image recognition at scale. In *International Conference on Learning Representations*, 2020.

[16] Samuel G Finlayson, John D Bowers, Joichi Ito, Jonathan L Zittrain, Andrew L Beam, and Isaac S Kohane. Adversarial attacks on medical machine learning. *Science*, pages 1287–1289, 2019.

[17] Yue Gao, I Shumailov, Kassem Fawaz, and Nicolas Papernot. On the limitations of stochastic pre-processing defenses. In *Advances in Neural Information Processing Systems*, pages 24280–24294, 2022.

[18] Ian J Goodfellow, Jonathon Shlens, and Christian Szegedy. Explaining and harnessing adversarial examples. In *International Conference on Learning Representations*, 2015.

[19] Alexandros Graikos, Nikolay Malkin, Nebojsa Jojic, and Dimitris Samaras. Diffusion models as plug-and-play priors. In *Advances in Neural Information Processing Systems*, pages 14715–14728, 2022.

[20] Will Grathwohl, Kuan-Chieh Wang, Joern-Henrik Jacobsen, David Duvenaud, Mohammad Norouzi, and Kevin Swersky. Your classifier is secretly an energy based model and you should treat it like one. In *International Conference on Learning Representations*, 2019.

[21] Kaiming He, Xiangyu Zhang, Shaoqing Ren, and Jian Sun. Deep residual learning for image recognition. In *Proceedings of the IEEE/CVF Conference on Computer Vision and Pattern Recognition*, pages 770–778, 2016.

[22] Jonathan Ho and Tim Salimans. Classifier-free diffusion guidance. In *NeurIPS 2021 Workshop on Deep Generative Models and Downstream Applications*, 2021.

[23] Jonathan Ho, Ajay Jain, and Pieter Abbeel. Denoising diffusion probabilistic models. *Advances in Neural Information Processing Systems*, pages 6840–6851, 2020.

[24] Pengfei Jing, Qiyi Tang, Yuefeng Du, Lei Xue, Xiapu Luo, Ting Wang, Sen Nie, and Shi Wu. Too good to be safe: Tricking lane detection in autonomous driving with crafted perturbations. In *Proceedings of USENIX Security Symposium*, pages 3237–3254, 2021.

[25] Diederik Kingma, Tim Salimans, Ben Poole, and Jonathan Ho. Variational diffusion models. *Advances in Neural Information Processing Systems*, pages 21696–21707, 2021.

[26] Alex Krizhevsky, Vinod Nair, and Geoffrey Hinton. The cifar-10 dataset. *online: http://www. cs. toronto. edu/kriz/cifar. html*, 55(5), 2014.

[27] Alex Krizhevsky, Ilya Sutskever, and Geoffrey E Hinton. Imagenet classification with deep convolutional neural networks. *Communications of the ACM*, pages 84–90, 2017.

[28] Cassidy Laidlaw, Sahil Singla, and Soheil Feizi. Perceptual adversarial robustness: Defense against unseen threat models. In *International Conference on Learning Representations*, 2021.

[29] Yann LeCun, Sumit Chopra, Raia Hadsell, M Ranzato, and Fujie Huang. A tutorial on energy-based learning. *Predicting structured data*, 1(0), 2006.

[30] Alexander C Li, Mihir Prabhudesai, Shivam Duggal, Ellis Brown, and Deepak Pathak. Your diffusion model is secretly a zero-shot classifier. *arXiv preprint arXiv:2303.16203*, 2023.

[31] Yingzhen Li, John Bradshaw, and Yash Sharma. Are generative classifiers more robust to adversarial attacks? In *International Conference on Machine Learning*, pages 3804–3814, 2019.

[32] Fangzhou Liao, Ming Liang, Yinpeng Dong, Tianyu Pang, Xiaolin Hu, and Jun Zhu. Defense against adversarial attacks using high-level representation guided denoiser. In *Proceedings of the IEEE/CVF Conference on Computer Vision and Pattern Recognition*, pages 1778–1787, 2018.

[33] Ze Liu, Yutong Lin, Yue Cao, Han Hu, Yixuan Wei, Zheng Zhang, Stephen Lin, and Baining Guo. Swin transformer: Hierarchical vision transformer using shifted windows. In *Proceedings of the IEEE/CVF International Conference on Computer Vision*, pages 10012–10022, 2021.

[34] Aleksander Madry, Aleksandar Makelov, Ludwig Schmidt, Dimitris Tsipras, and Adrian Vladu. Towards deep learning models resistant to adversarial attacks. In *International Conference on Learning Representations*, 2018.

[35] Andrew Y Ng and Michael I Jordan. On discriminative vs. generative classifiers: a comparison of logistic regression and naive bayes. In *Proceedings of the 14th International Conference on Neural Information Processing Systems: Natural and Synthetic*, pages 841–848, 2001.

[36] Alexander Quinn Nichol and Prafulla Dhariwal. Improved denoising diffusion probabilistic models. In *International Conference on Machine Learning*, pages 8162–8171, 2021.

[37] Weili Nie, Brandon Guo, Yujia Huang, Chaowei Xiao, Arash Vahdat, and Animashree Anandkumar. Diffusion models for adversarial purification. In *International Conference on Machine Learning*, pages 16805–16827, 2022.

[38] Aditi Raghunathan, Jacob Steinhardt, and Percy Liang. Certified defenses against adversarial examples. In *International Conference on Learning Representations*, 2018.

[39] Rajat Raina, Yirong Shen, Andrew Y Ng, and Andrew McCallum. Classification with hybrid generative/discriminative models. In *Proceedings of the 16th International Conference on Neural Information Processing Systems*, pages 545–552, 2003.

[40] Sylvestre-Alvise Rebuffi, Sven Gowal, Dan A Calian, Florian Stimberg, Olivia Wiles, and Timothy Mann. Fixing data augmentation to improve adversarial robustness. *arXiv preprint arXiv:2103.01946*, 2021.

[41] Olga Russakovsky, Jia Deng, Hao Su, Jonathan Krause, Sanjeev Satheesh, Sean Ma, Zhiheng Huang, Andrej Karpathy, Aditya Khosla, Michael Bernstein, et al. Imagenet large scale visual recognition challenge. *International journal of computer vision*, 115(3):211–252, 2015.

[42] Pouya Samangouei, Maya Kabkab, and Rama Chellappa. Defense-gan: Protecting classifiers against adversarial attacks using generative models. In *International Conference on Learning Representations*, 2018.

[43] L Schott, J Rauber, M Bethge, and W Brendel. Towards the first adversarially robust neural network model on mnist. In *International Conference on Learning Representations*, 2019.

[44] Mahmood Sharif, Sruti Bhagavatula, Lujo Bauer, and Michael K. Reiter. Accessorize to a crime: Real and stealthy attacks on state-of-the-art face recognition. In *ACM Sigsac Conference on Computer and Communications Security*, pages 1528–1540, 2016.

[45] Jascha Sohl-Dickstein, Eric Weiss, Niru Maheswaranathan, and Surya Ganguli. Deep unsupervised learning using nonequilibrium thermodynamics. In *International Conference on Machine Learning*, pages 2256–2265, 2015.

[46] Jiaming Song, Chenlin Meng, and Stefano Ermon. Denoising diffusion implicit models. In *International Conference on Learning Representations*, 2020.

[47] Yang Song and Stefano Ermon. Generative modeling by estimating gradients of the data distribution. In *Proceedings of the 33rd International Conference on Neural Information Processing Systems*, pages 11918–11930, 2019.

[48] Yang Song, Taesup Kim, Sebastian Nowozin, Stefano Ermon, and Nate Kushman. Pixeldefend: Leveraging generative models to understand and defend against adversarial examples. In *International Conference on Learning Representations*, 2018.

[49] Yang Song, Jascha Sohl-Dickstein, Diederik P Kingma, Abhishek Kumar, Stefano Ermon, and Ben Poole. Score-based generative modeling through stochastic differential equations. In *International Conference on Learning Representations*, 2021.

[50] Yang Song, Prafulla Dhariwal, Mark Chen, and Ilya Sutskever. Consistency models. *arXiv preprint arXiv:2303.01469*, 2023.

[51] Christian Szegedy, Wojciech Zaremba, Ilya Sutskever, Joan Bruna, Dumitru Erhan, Ian Goodfellow, and Rob Fergus. Intriguing properties of neural networks. *International Conference on Learning Representations*, 2014.

[52] Florian Tramèr and Dan Boneh. Adversarial training and robustness for multiple perturbations. In *Proceedings of the 33rd International Conference on Neural Information Processing Systems*, pages 5866–5876, 2019.

[53] Florian Tramer, Nicholas Carlini, Wieland Brendel, and Aleksander Madry. On adaptive attacks to adversarial example defenses. In *Advances in Neural Information Processing Systems*, pages 1633–1645, 2020.

[54] Jinyi Wang, Zhaoyang Lyu, Dahua Lin, Bo Dai, and Hongfei Fu. Guided diffusion model for adversarial purification. *arXiv preprint arXiv:2205.14969*, 2022.

[55] Zekai Wang, Tianyu Pang, Chao Du, Min Lin, Weiwei Liu, and Shuicheng Yan. Better diffusion models further improve adversarial training. *arXiv preprint arXiv:2302.04638*, 2023.

[56] Eric Wong and Zico Kolter. Provable defenses against adversarial examples via the convex outer adversarial polytope. In *International Conference on Machine Learning*, pages 5286–5295, 2018.

[57] Chaowei Xiao, Jun-Yan Zhu, Bo Li, Warren He, Mingyan Liu, and Dawn Song. Spatially transformed adversarial examples. In *International Conference on Learning Representations*, 2018.

[58] Chaowei Xiao, Zhongzhu Chen, Kun Jin, Jiongxiao Wang, Weili Nie, Mingyan Liu, Anima Anandkumar, Bo Li, and Dawn Song. Densepure: Understanding diffusion models for adversarial robustness. In *International Conference on Learning Representations*, 2023.

[59] Xiulong Yang, Sheng-Min Shih, Yinlin Fu, Xiaoting Zhao, and Shihao Ji. Your vit is secretly a hybrid discriminative-generative diffusion model. *arXiv preprint arXiv:2208.07791*, 2022.

[60] Sergey Zagoruyko and Nikos Komodakis. Wide residual networks. In *British Machine Vision Conference 2016*, pages 87.1–87.12, 2016.

[61] Hongyang Zhang, Yaodong Yu, Jiantao Jiao, Eric Xing, Laurent El Ghaoui, and Michael Jordan. Theoretically principled trade-off between robustness and accuracy. In *International Conference on Machine Learning*, pages 7472–7482, 2019.

[62] Roland S Zimmermann, Lukas Schott, Yang Song, Benjamin Adric Dunn, and David A Klindt. Score-based generative classifiers. In *NeurIPS 2021 Workshop on Deep Generative Models and Downstream Applications*, 2021.

A Proof of Theorem 3.1

Proof.

$$
\begin{aligned}
p_\theta(y|\mathbf{x}) &= \frac{p_\theta(\mathbf{x}, y)}{\sum_{\hat{y}} p_\theta(\mathbf{x}, \hat{y})} \\
&= \frac{p_\theta(\mathbf{x}|y)p_\theta(y)}{\sum_{y} p_\theta(\mathbf{x}|\hat{y})p_\theta(\hat{y})} \\
&= \frac{p_\theta(\mathbf{x}|y)}{\sum_{\hat{y}} p_\theta(\mathbf{x}|\hat{y})} \\
&= \frac{e^{\log p_\theta(\mathbf{x}|y)}}{\sum_{\hat{y}} e^{\log p_\theta(\mathbf{x}|\hat{y})}} \\
&= \frac{\exp\Big(\mathbb{E}_{\boldsymbol{\epsilon},t}[w_t\|\boldsymbol{\epsilon}_\theta(\mathbf{x}_t, t, y) - \boldsymbol{\epsilon}\|_2^2] + \log p_\theta(\mathbf{x}|y) - \mathbb{E}_{\boldsymbol{\epsilon},t}[w_t\|\boldsymbol{\epsilon}_\theta(\mathbf{x}_t, t, y) - \boldsymbol{\epsilon}\|_2^2]\Big)}{\sum_{\hat{y}} \exp\Big(\mathbb{E}_{\boldsymbol{\epsilon},t}[w_t\|\boldsymbol{\epsilon}_\theta(\mathbf{x}_t, t, \hat{y}) - \boldsymbol{\epsilon}\|_2^2] + \log p_\theta(\mathbf{x}|\hat{y}) - \mathbb{E}_{\boldsymbol{\epsilon},t}[w_t\|\boldsymbol{\epsilon}_\theta(\mathbf{x}_t, t, \hat{y}) - \boldsymbol{\epsilon}\|_2^2]\Big)} \\
&= \frac{\exp\Big(\mathbb{E}_{\boldsymbol{\epsilon},t}[w_t\|\boldsymbol{\epsilon}_\theta(\mathbf{x}_t, t, y) - \boldsymbol{\epsilon}\|_2^2] + \log p_\theta(\mathbf{x}|y)\Big)\exp\Big(-\mathbb{E}_{\boldsymbol{\epsilon},t}[w\|\boldsymbol{\epsilon}_\theta(\mathbf{x}_t, t, y) - \boldsymbol{\epsilon}\|_2^2]\Big)}{\sum_{\hat{y}} \exp\Big(\mathbb{E}_{\boldsymbol{\epsilon},t}[w_t\|\boldsymbol{\epsilon}_\theta(\mathbf{x}_t, t, \hat{y}) - \boldsymbol{\epsilon}\|_2^2] + \log p_\theta(\mathbf{x}|\hat{y})\Big)\exp\Big(-\mathbb{E}_{\boldsymbol{\epsilon},t}[w_t\|\boldsymbol{\epsilon}_\theta(\mathbf{x}_t, t, \hat{y}) - \boldsymbol{\epsilon}\|_2^2]\Big)}.
\end{aligned}
$$

When $\forall \hat{y},\ d(\mathbf{x}, \hat{y}, \theta) \to 0$, we can get:

$$
\forall \hat{y},\ \exp\Big(\mathbb{E}_{\boldsymbol{\epsilon},t}[w_t\|\boldsymbol{\epsilon}_\theta(\mathbf{x}_t, t, \hat{y}) - \boldsymbol{\epsilon}\|_2^2] + \log p_\theta(\mathbf{x}|\hat{y})\Big) \to 1.
$$

Therefore,

$$
p_\theta(y|\mathbf{x}) = \frac{\exp\Big(-\mathbb{E}_{\boldsymbol{\epsilon},t}[w_t\|\boldsymbol{\epsilon}_\theta(\mathbf{x}_t, t, y) - \boldsymbol{\epsilon}\|_2^2]\Big)}{\sum_{\hat{y}} \exp\Big(-\mathbb{E}_{\boldsymbol{\epsilon},t}[w_t\|\boldsymbol{\epsilon}_\theta(\mathbf{x}_t, t, \hat{y}) - \boldsymbol{\epsilon}\|_2^2]\Big)}.
$$

□

B Derivation of the optimal diffusion classifier

B.1 Optimal diffusion model: proof of Theorem 3.2

Proof. The optimal diffusion model has the minimal error $\mathbb{E}_{\mathbf{x},t,y}[\|\boldsymbol{\epsilon}(\mathbf{x}_t, t, y) - \boldsymbol{\epsilon}\|_2^2]$ among all the models in hypothesis space. Since the prediction for one input pair $(\mathbf{x}_t, t, y)$ does not affect the prediction for any other input pairs, the optimal diffusion model will give the optimal solution for any input pair $(\mathbf{x}_t, t, y)$:

$$
\mathbb{E}_{\mathbf{x}^{(i)}\sim p(\mathbf{x}^{(i)}|\mathbf{x}_t,y)}[\|\boldsymbol{\epsilon}_{\theta^*_D}(\mathbf{x}_t, t, y) - \boldsymbol{\epsilon}_i\|_2^2] = \min_\theta \mathbb{E}_{\mathbf{x}^{(i)}\sim p(\mathbf{x}^{(i)}|\mathbf{x}_t,y)}[\|\boldsymbol{\epsilon}_\theta(\mathbf{x}_t, t, y) - \boldsymbol{\epsilon}_i\|_2^2],
$$

where $\boldsymbol{\epsilon}_i = \frac{\mathbf{x}_t - \sqrt{\alpha_t}\mathbf{x}^{(i)}}{\sigma_t}$.

Note that

$$
p(\mathbf{x}^{(i)}|\mathbf{x}_t, y) = \frac{p(\mathbf{x}^{(i)}|y)p(\mathbf{x}_t|\mathbf{x}^{(i)}, y)}{p(\mathbf{x}_t|y)} = \frac{p(\mathbf{x}^{(i)}|y)q(\mathbf{x}_t|\mathbf{x}^{(i)})}{p(\mathbf{x}_t|y)}.
$$

Assume that

$$
p(\mathbf{x}^{(i)}|y) = \begin{cases} \frac{1}{|D_y|} & , \mathbf{x}^{(i)} \in D_y \\ 0 & , \mathbf{x}^{(i)} \notin D_y \end{cases}
$$

Solving $\frac{\partial}{\partial \boldsymbol{\epsilon}_\theta(\mathbf{x}_t,t,y)} \mathbb{E}_{\mathbf{x}^{(i)}\sim p(\mathbf{x}^{(i)}|\mathbf{x}_t,y)}[\|\boldsymbol{\epsilon}_\theta(\mathbf{x}_t, t, y) - \boldsymbol{\epsilon}_i\|_2^2] = 0$, we can get:

$$\mathbb{E}_{\mathbf{x}^{(i)}\sim p(\mathbf{x}^{(i)}|\mathbf{x}_t,y)}[\boldsymbol{\epsilon}_\theta(\mathbf{x}_t,t,y)-\boldsymbol{\epsilon}_i]=0,$$
$$\sum_{x^{(i)}\in D} p(\mathbf{x}^{(i)}|\mathbf{x}_t,y)\boldsymbol{\epsilon}_\theta(\mathbf{x}_t,t,y)=\boldsymbol{\epsilon}_\theta(\mathbf{x}_t,t,y)=\sum_{\mathbf{x}^{(i)}\in D_y} p(\mathbf{x}^{(i)}|\mathbf{x}_t,y)\boldsymbol{\epsilon}_i.$$

Substitute $\boldsymbol{\epsilon}_i$ by Eq. (1):

$$\begin{aligned}
\boldsymbol{\epsilon}_\theta(\mathbf{x}_t,t,y) &= \sum_{\mathbf{x}^{(i)}\in D_y} p(\mathbf{x}^{(i)}|\mathbf{x}_t,y)\frac{\mathbf{x}_t-\sqrt{\alpha_t}\mathbf{x}^{(i)}}{\sigma_t}\\
&= \sum_{\mathbf{x}^{(i)}\in D_y} \frac{p(\mathbf{x}^{(i)}|y)q(\mathbf{x}_t|\mathbf{x}^{(i)})}{p(\mathbf{x}_t|y)}\frac{\mathbf{x}_t-\sqrt{\alpha_t}\mathbf{x}^{(i)}}{\sigma_t}\\
&= \sum_{\mathbf{x}^{(i)}\in D_y} \frac{p(\mathbf{x}^{(i)}|y)}{p(\mathbf{x}_t|y)}p(\mathcal{N}(\mathbf{x}_t|\sqrt{\alpha_t}\mathbf{x}^{(i)},\sigma_t^2 I)=\frac{\mathbf{x}_t-\sqrt{\alpha_t}\mathbf{x}^{(i)}}{\sigma_t})\frac{\mathbf{x}_t-\sqrt{\alpha_t}\mathbf{x}^{(i)}}{\sigma_t}\\
&= \sum_{\mathbf{x}^{(i)}\in D_y} \frac{p(\mathbf{x}^{(i)}|y)}{p(\mathbf{x}_t|y)}\frac{1}{(2\pi\sigma_t)^{\frac{n}{2}}}\exp\left(-\frac{\|\mathbf{x}_t-\sqrt{\alpha_t}\mathbf{x}^{(i)}\|_2^2}{2\sigma_t^2}\right)\frac{\mathbf{x}_t-\sqrt{\alpha_t}\mathbf{x}^{(i)}}{\sigma_t}
\end{aligned}$$

To avoid numerical problem caused by $\frac{1}{(2\pi\sigma_t)^{\frac{n}{2}}}$ and intractable $\frac{p(\mathbf{x}^{(i)}|y)}{p(\mathbf{x}_t|y)}$, we re-organize this equation using softmax function:

$$\begin{aligned}
\boldsymbol{\epsilon}_\theta(\mathbf{x}_t,t,y) &= \sum_{\mathbf{x}^{(i)}\in D_y} \frac{\frac{p(\mathbf{x}^{(i)}|y)}{p(\mathbf{x}_t|y)}\frac{1}{(2\pi\sigma_t)^{\frac{n}{2}}}\exp\left(-\frac{\|\mathbf{x}_t-\sqrt{\alpha_t}\mathbf{x}^{(i)}\|_2^2}{2\sigma_t^2}\right)}{\sum_{i=j}^{|D_y|}p(\mathbf{x}_j|\mathbf{x}_t,y)}\frac{\mathbf{x}_t-\sqrt{\alpha_t}\mathbf{x}^{(i)}}{\sigma_t}\\
&= \sum_{\mathbf{x}^{(i)}\in D_y} \frac{\frac{p(\mathbf{x}^{(i)}|y)}{p(\mathbf{x}_t|y)}\frac{1}{(2\pi\sigma_t)^{\frac{n}{2}}}\exp\left(-\frac{\|\mathbf{x}_t-\sqrt{\alpha_t}\mathbf{x}^{(i)}\|_2^2}{2\sigma_t^2}\right)}{\sum_{j=1}^{|D_y|}\frac{p(\mathbf{x}_j|y)}{p(\mathbf{x}_t|y)}\frac{1}{(2\pi\sigma_t)^{\frac{n}{2}}}\exp\left(-\frac{\|\mathbf{x}_t-\sqrt{\alpha_t}\mathbf{x}_j\|_2^2}{2\sigma_t^2}\right)}\frac{\mathbf{x}_t-\sqrt{\alpha_t}\mathbf{x}^{(i)}}{\sigma_t}\\
&= \sum_{\mathbf{x}^{(i)}\in D_y} \frac{1}{\sigma_t}(\mathbf{x}_t-\sqrt{\alpha_t}\mathbf{x}^{(i)})\text{softmax}(-\frac{1}{2\sigma_t^2}\|\mathbf{x}_t-\sqrt{\alpha_t}\mathbf{x}^{(i)}\|_2^2).
\end{aligned}$$

This is the result of Eq. (7). □

B.2 Optimal diffusion classifier: proof of Theorem 3.3

Proof. Substitute Eq. (7) into Eq. (6):

$$\begin{aligned}
f_{\theta_D^*}(\mathbf{x})_y &= -\mathbb{E}_{\boldsymbol{\epsilon},t}[\|\boldsymbol{\epsilon}_\theta(\mathbf{x}_t,t,y)-\boldsymbol{\epsilon}\|_2^2]\\
&= -\mathbb{E}_{t,\boldsymbol{\epsilon}}[\|\sum_{\mathbf{x}^{(i)}\in D_y}[\frac{1}{\sigma_t}(\mathbf{x}_t-\sqrt{\alpha_t}\mathbf{x}^{(i)})\text{softmax}(-\frac{1}{2\sigma_t^2}\|\mathbf{x}_t-\sqrt{\alpha_t}\mathbf{x}^{(i)}\|_2^2)]-\boldsymbol{\epsilon}\|_2^2]\\
&= -\mathbb{E}_{t,\boldsymbol{\epsilon}}[\|\sum_{\mathbf{x}^{(i)}\in D_y}[\frac{1}{\sigma_t}(\sqrt{\alpha_t}\mathbf{x}+\sigma_t\boldsymbol{\epsilon}-\sqrt{\alpha_t}\mathbf{x}^{(i)})\text{softmax}(-\frac{1}{2\sigma_t^2}\|\sqrt{\alpha_t}\mathbf{x}+\sigma_t\boldsymbol{\epsilon}-\sqrt{\alpha_t}\mathbf{x}^{(i)}\|_2^2)-\boldsymbol{\epsilon}\|_2^2]\\
&= -\mathbb{E}_{t,\boldsymbol{\epsilon}}[\|\sum_{\mathbf{x}^{(i)}\in D_y}[\frac{1}{\sigma_t}(\sqrt{\alpha_t}\mathbf{x}-\sqrt{\alpha_t}\mathbf{x}^{(i)})\text{softmax}(-\frac{1}{2\sigma_t^2}\|\sqrt{\alpha_t}\mathbf{x}+\sigma_t\boldsymbol{\epsilon}-\sqrt{\alpha_t}\mathbf{x}^{(i)}\|_2^2)\\
&+\boldsymbol{\epsilon}\sum_{\mathbf{x}^{(i)}\in D_y}\text{softmax}(-\frac{1}{2\sigma_t^2}\|\sqrt{\alpha_t}\mathbf{x}+\sigma_t\boldsymbol{\epsilon}-\sqrt{\alpha_t}\mathbf{x}^{(i)}\|_2^2)-\boldsymbol{\epsilon}]\|_2^2]\\
&= -\mathbb{E}_{t,\boldsymbol{\epsilon}}[\|\sum_{\mathbf{x}^{(i)}\in D_y}[\frac{1}{\sigma_t}(\sqrt{\alpha_t}\mathbf{x}-\sqrt{\alpha_t}\mathbf{x}^{(i)})s(\mathbf{x},\mathbf{x}^{(i)},\boldsymbol{\epsilon},t)]\|_2^2]\\
&= -\mathbb{E}_{\boldsymbol{\epsilon},t}[\frac{\alpha_t}{\sigma_t^2}\|\sum_{\mathbf{x}^{(i)}\in D_y}s(\mathbf{x},\mathbf{x}^{(i)},\boldsymbol{\epsilon},t)(\mathbf{x}-\mathbf{x}^{(i)})\|_2^2].
\end{aligned}$$

We get the result. □

C More experimental results

C.1 Computational resources

We conduct Direct Attack on 4× A100 GPUs due to the large memory cost of computational graphs for second-order derivatives. We use 12× 3090 GPUs for other experiments.

C.2 ℓ_2 robustness

In this section, we adapt our RDC to the ℓ_2 threat model. We only modify the optimization budget η to 0.5 under the ℓ_2 norm. We achieve 95.86% accuracy on clean images and 84.37% under adaptive attacks, comparable with state-of-the-art adversarial training models in Table 1.

D Connection between Energy-Based Models (EBMs)

The EBMs [29] directly use neural networks to learn $p_\theta(\mathbf{x})$ and $p_\theta(\mathbf{x}|y)$.

$$p_\theta(\mathbf{x}|y) = \frac{\exp(-E_\theta(\mathbf{x})_y)}{Z(\theta, y)},$$

Where $E_\theta(\mathbf{x}) : R^D \to R^n$, and $Z(\theta, y) = \int \exp(-E_\theta(\mathbf{x})_y) d\mathbf{x}$ is the normalizing constant.

As described in [20], we can use EBMs to classify images by calculating the conditional probability:

$$p_\theta(y|\mathbf{x}) = \frac{\exp(-E_\theta(\mathbf{x})_y)}{\sum_{\hat{y}} \exp(-E_\theta(\mathbf{x})_{\hat{y}})} \tag{11}$$

Compare Eq. (11) and Eq. (6), we can also set the energy function as:

$$E_\theta(\mathbf{x})_y \approx \mathbb{E}_{t,\boldsymbol{\epsilon}} \left[w_t \|\boldsymbol{\epsilon}_\theta(\mathbf{x}_t, t, y) - \boldsymbol{\epsilon}\|_2^2 \right] \tag{12}$$

Therefore, our diffusion classifier could be viewed as an EBM, and the energy function is the conditional diffusion loss.